

## Clouds, fibres and echoes: a new approach to studying random walks on fractals

This article has been downloaded from IOPscience. Please scroll down to see the full text article.

2001 J. Phys. A: Math. Gen. 34 L289

(<http://iopscience.iop.org/0305-4470/34/20/101>)

View [the table of contents for this issue](#), or go to the [journal homepage](#) for more

Download details:

IP Address: 171.66.16.95

The article was downloaded on 02/06/2010 at 08:58

Please note that [terms and conditions apply](#).

## LETTER TO THE EDITOR

# Clouds, fibres and echoes: a new approach to studying random walks on fractals

M Davison<sup>1</sup>, C Essex<sup>1</sup>, C Schulzky<sup>2</sup>, A Franz<sup>2</sup> and K H Hoffmann<sup>2</sup>

<sup>1</sup> Department of Applied Mathematics, The University of Western Ontario, London, Canada N6A 5B7

<sup>2</sup> Institut für Physik, Technische Universität, D-09107 Chemnitz, Germany

Received 17 July 2000, in final form 12 April 2001

## Abstract

Up to now the general approach of constructing evolution differential equations to describe random walks on fractals has not succeeded. Is this because the true probability density function is inherently fractal? When plotted in the appropriate similarity variable, we find a cloud which is not too smooth. Further investigation shows that this cloud has a structure that might be overlooked if one is looking for the usual single-valued probability density function. The cloud is composed of an infinite family of smooth fibres, each of which describes the behaviour of the walk on an infinite echo point class. The fibres are individually smooth and so are naturally amenable to analysis with differential equations.

PACS numbers: 0545D, 6610C, 0540F

## 1. Introduction

Even though they are not differentiable, fractals can arise from differential equations. The Lorenz attractor is a well known example. Do differential equations arise from fractals? Clearly from fractals alone the answer is no, however the random walks on fractals, frequently used to provide a model for anomalous diffusion, are a different matter. So can differential equations arise from dynamics on fractals?

A number of attempts [1–5] have been made to provide differential or integro-differential equations to explore anomalous diffusion, mostly as a random walk on a Sierpinski gasket. These have only been partially successful. Our findings [5] suggest that alternative strategies may be needed. This letter presents one possible alternative.

The diffusion or heat partial differential equation has long been used to study random walks on Euclidean lattices. Several papers [1–5] attempt to generalize this relationship to find evolution equations which describe the statistical behaviour of random walks on fractals. This is interesting because of its link to anomalous diffusion. These papers are considered in [5] and their predictions are compared with the statistical behaviour observed from a random walk on a Sierpinski gasket. The predicted behaviours each capture something of the observed statistical behaviour, but none captures it all.

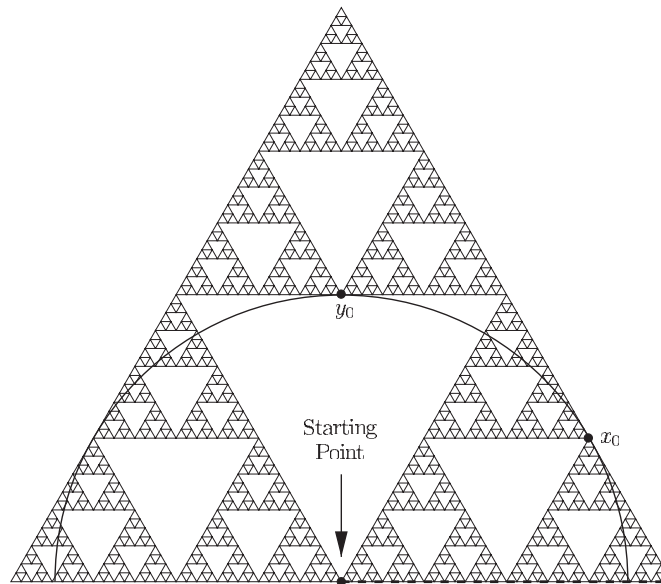


**Figure 1.** 7th iteration of the Sierpinski gasket. Note the points  $x_0$  and  $y_0$  at the same radius, and the dashed line denoting the ray for figure 2.

The problem might not simply be that the correct evolution equation has just not yet been found—it could be much more fundamental. The sticking point could be that fractals are, by definition, ‘spiky’ or ‘rough’. As a result they, or walks upon them, do not lend themselves to description by differential or integral equations, which require a certain degree of smoothness to work. A way around this rather obvious difficulty is to look at some type of averaged quantity—but what type of averaging? For a random walk on a fractal, for instance, the number of walkers that have travelled a radial distance of  $r$  from the starting point in a time  $t$ , is collected to obtain the probability density function  $P(r, t)$ . This type of angular averaging does not impart enough smoothness [1, 5], so  $P(r, t)$  remains fractal like. We do not know the dynamics of the random walk well enough to perform the kind of physically meaningful averaging needed for smoothness. So far, averaging, as a concept, seems at its best to be *ad hoc*.

In this letter we return to the example of a random walk on a relatively simple fractal—the Sierpinski gasket—to experimentally determine more about the dynamics of random walks on fractals. We use the natural similarity group of the walk to find interesting structure in random-walk behaviour not previously documented. We describe the structure observed from that viewpoint in terms of ‘muscles’ and ‘fibres’. These ‘fibres’, which turn out to be smooth functions, might provide the solution to the long-standing problem of determining some evolution integro-differential equation which describes random walks on fractals.

## 2. Numerical simulation

We present results obtained in studying a random walk on a Sierpinski gasket. Our numerical method follows that of [6]. We construct finitely generated Sierpinski gaskets of depth 10–12 and then inject a walker into each of them at the centre of the bottom face of the biggest triangle (see figure 1). Lattice sites are located at vertices. At each time step a walker is equally likely

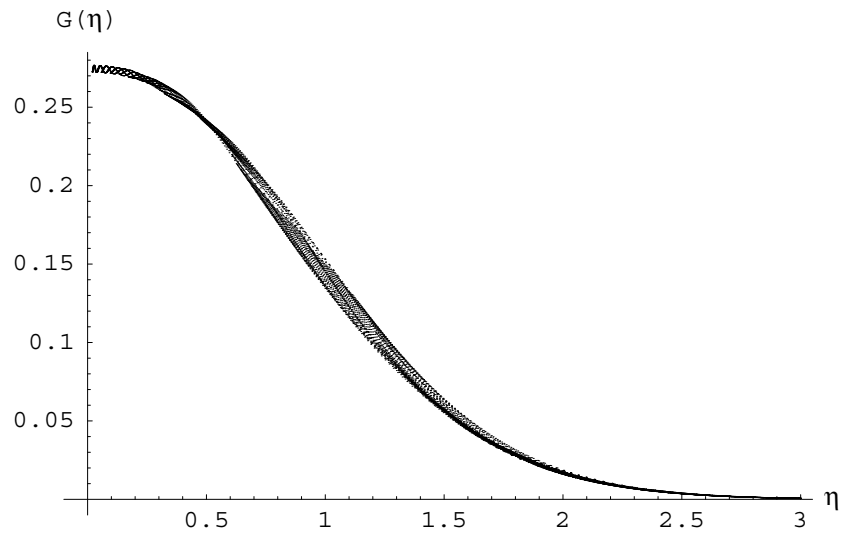


Figure 2. The computed GDF data for all points of the gasket along the ray indicated in figure 1.

to move to any of the lattice sites joined to its present location. These moving rules are encoded using a master equation formalism.

How do we display the data so obtained? We could assign cartesian coordinates to each vertex on the finitely generated gasket and plot  $P(x, y, t)$ , the probability to find a walker at the point  $(x, y)$  at time  $t$ . We hope that  $P$  is one element in a sequence of functions, defined for each iteration depth, with the limit being a map  $\mathcal{F} \times \mathcal{R}^+ \rightarrow \mathcal{R}^+$ , where  $\mathcal{F}$  is the fractal set of the points contained in the Sierpinski gasket. While topological ideas of continuity could be used to describe this mapping, this is not the approach typically adopted by workers in this area.

The traditional quantity to be measured is the radial distance from the starting point travelled by a walker. Typically the distance from a site to the injection point is calculated and the probability distribution at points along a fixed representative ray from the injection point, is plotted as a function of  $r$ . This new simpler probability is a map  $\mathcal{R}^+ \times \mathcal{R}^+ \rightarrow \mathcal{R}^+$ . However, because the fractal is not isotropic about the origin the function corresponding to one particular ray will differ from those corresponding to other rays. That means that this common practice does not produce a single-valued function. We accept these resulting multi-valued functions in order to conform to standard practice. To simplify plotting and comparisons, we may use the similarity solution method expounded in [7] and [5], and note that this method suggests for any PDF with the correct scaling

$$P(r, t) = t^{-\frac{d_f}{d_w}} G(\eta) \tag{1a}$$

where  $d_f$  is the fractal dimension,  $d_w$  is the walk dimension, and

$$\eta = \frac{r}{t^{\frac{1}{d_w}}}. \tag{1b}$$

It is better to plot  $G(\eta)$  (which we call the GDF) than  $P(r, t)$ : (1a) tells us how to create  $P(r, t)$  from  $G(\eta)$ ,  $G(\eta)$  has all the information we require, and it is easier to look at a 2D rather than a 3D plot. There is also a deeper advantage to considering  $G(\eta)$  which will become evident later.

An example of such a GDF plot can be constructed along the horizontal ray indicated by the dashed horizontal line seen in figure 1. This is similar to the one used in [1]. Figure 2 is

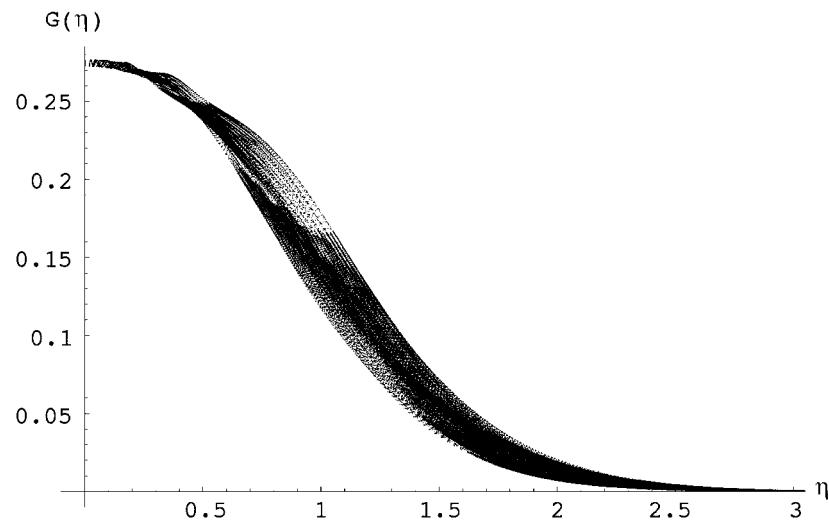


**Figure 3.** The computed GDF data for all points of the whole gasket. This ‘cloud’ contains the points plotted in figure 2 as a subset.

the resulting GDF plot, which exhibits the indicated multi-valued character in the form of a cloud of points. That is the data points do not fall onto a simple curve, instead they appear to fall on a ‘muscle’-like cloud. It should be noted that this observation is consistent with the similarity group as the entire cloud scales in accordance with that group. But, if our objective is the creation of an evolution equation for  $G$ , this observation is disappointing as it suggests either the presence of a solution which appears extremely oscillatory or even fractal. But the situation is actually worse than these as many values of  $\eta$  have more than one data value! This is in contrast to the normal single-valued theoretical GDFs arising from the differential equations designed to model this process [5].

This is perhaps the most compelling reason why a direct treatment of these types of densities has not worked. Of course one can imagine that these multiple values and wild fluctuations can be averaged away, but that process begs several questions. The first is *why* an average is justified in the first place—there is no significant observation error here. Moreover no physical basis has been proposed to expect that instruments will average over the multiple values in practice. Then the second question is *what form* would any such proposed process of averaging take. A similar set of questions arise for the problem of averaging over initial conditions. We agree that investigating the effect of such averaging is interesting, but concentrate here on studying the dispersion of a point source of walkers. We are led to study this more restrictive problem by the fact that existing PDE-based models of anomalous diffusion have failed to explain simulations [5]. It is by no means clear how to answer these questions, so we adopt a different approach.

It is motivated by a key observation—the muscle-like cloud appears to be the assembly of a number of curves on which data fall. We name these curves ‘fibres’, in keeping with our ‘muscle’ analogy. In the next section the ‘fibres’ will be explained in terms of sets of ‘echo points’ induced by the similarity group described in (1b). It will be shown that use of this ‘echo point set’ will allow the production of smooth GDF curves whose physical interpretation is unambiguous.

Figure 3 shows data from all points computed on the fractal, which is in effect the plotting

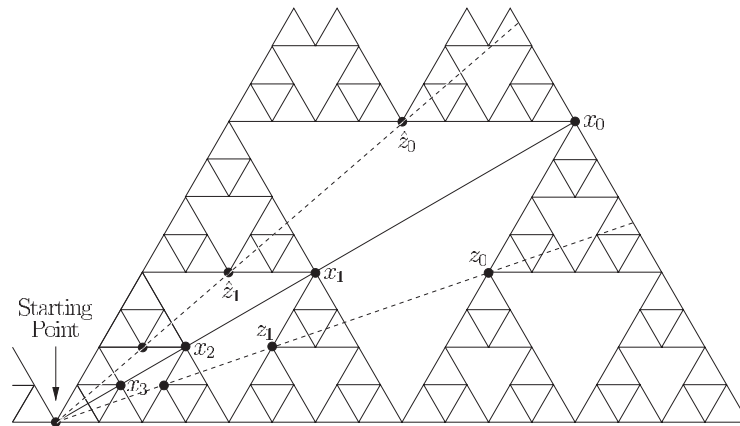


**Figure 4.** A few members of three different classes of echo points  $\{x_k\}$ ,  $\{z_k\}$   $\{\hat{z}_k\}$  are represented on a gasket schematic. The  $x_k$  are situated along a symmetry line, while the points  $z_k$  and  $\hat{z}_k$  are reflections of each other about that line.

of data along all rays. Clearly the structure of a muscle-like cloud and the fibrous appearance is fully retained although it is somewhat thickened. That is because the fibres from figure 2 are necessarily a subset of those in figure 3. The structure of the muscle in figure 3 will be discussed further below.

In passing we note that the envelope of the cloud in figures 2 and 3 seems to display ‘wiggles’ for small  $\eta$ . In fact these wiggles turn out to be intrinsic to individual fibres and they appear to be log-periodic in  $\eta$ . Similar sorts of behaviour have been noted in [8–10].

### 3. Fibres

To understand the fibres, we use the idea of fixing a reference point  $y$  on the fractal and sampling the PDF there over time. In the  $\eta$ , or similarity space, this corresponds to visiting all values of  $\eta$  corresponding to that reference point over different times. In this way we can associate an entire  $G_y(\eta)$  curve—which turns out to be one of the fibres in the  $G(\eta)$  cloud—with each point on the fractal. These curves are then shown to be continuous and smooth. In the following we skip the index ‘ $y$ ’ at  $G_y(\eta)$ .

What we shall now show is that some pairs of points on the fractal cast up identical  $G(\eta)$  curves, while other pairs represent different curves. Our description depends on figures 1 and 4.

To begin, focus attention, for example, on the pair of points  $x_1$  and  $x_2$  in figure 4. The point  $x_1$  is at the apex of a triangle with  $x_2$  at its base.  $x_2$  is also at the apex of a corresponding triangle half as large. If figure 4 was not just a schematic, all of the triangles of the gasket in the neighbourhood of  $x_2$  would be half of the corresponding ones in the neighbourhood of  $x_1$ . All the distances between points are thus scaled by a factor of 2. As this is exactly what the similarity transformation (1b) describes. Using (1b) we can quickly see, recalling that  $d_w = \frac{\ln 5}{\ln 2}$ , that

$$\eta(x_1, 5t) = \eta(x_2, t).$$

This tells us that every point in the  $\eta$  space induced by  $x_2$  also shows up in the  $\eta$  space induced by  $x_1$ . Furthermore, the fact that  $x_1$  and  $x_2$  play identical roles, up to a change of scale, in the gasket implies that the similarity scaling argument for the PDFs evaluated at those points also

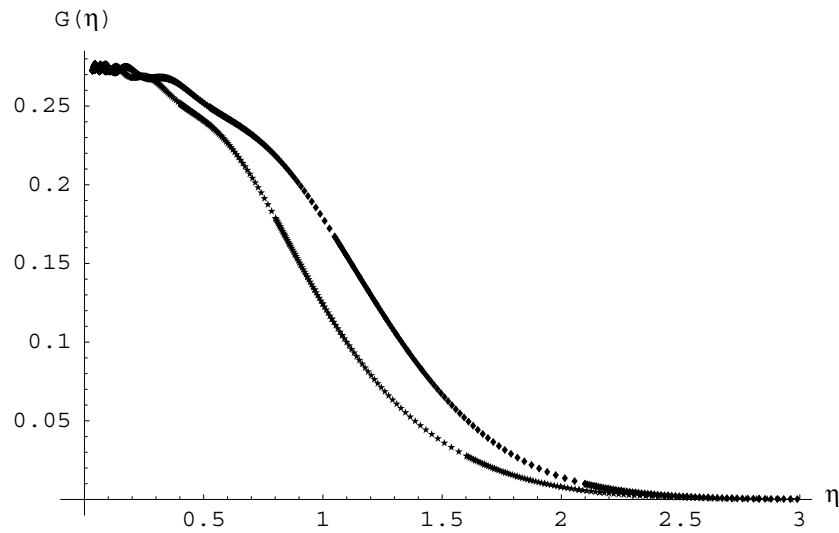


Figure 5. Fibre  $G$ 's corresponding to  $\{x_k\}$  (diamonds) and  $\{z_k\}$  (stars) echo classes.

applies, so that

$$P(x_1, 5t) = t^{\frac{d_t}{d_w}} P(x_2, t).$$

Because of this,

$$G(\eta_{1,5t}) = G(\eta_{2,t})$$

where

$$\eta_{k,t} = \frac{x_k}{t^{\frac{1}{d_w}}}.$$

Therefore the GDF created by waiting at the point  $x_1$  and monitoring the PDF is identical to that created by waiting at point  $x_2$ . Furthermore, on the solid line, the point  $x_3$  and all the other implied sequential points,  $x_k$ , which are suppressed in the figure 4 schematic for clarity, generate the same GDF. We call a set of points like  $(x_k)_{k=0}^{\infty}$  an *echo class*, while the sequence of points  $(z_k)_{k=0}^{\infty}$ , similarly represented in figure 4, constitutes a different echo class.

We name the GDF induced by a given echo class a *fibre*. The fibres corresponding to the  $x_k$  and  $z_k$  are shown in figure 5. We see there that for the computation not every pair of points has the same  $G(\eta)$  function. It is easy to see that this is true in principle too. Consider the points  $x_0$  and  $y_0$  in figure 1. Since  $x_0$  and  $y_0$  are the same distance from the origin, at any given time  $t^*$ ,  $\eta(x_0, t^*) = \eta(y_0, t^*)$ . However,  $P(x_0, t^*)$  is generally not the same as  $P(y_0, t^*)$ . This proves that these two points induce *different* GDF curves. Note that members of two different echo classes can for symmetry reasons yield the same fibre. See, for example, the points  $\hat{z}_k$  and  $z_k$  in figure 4.

The points that are plotted in the  $G(\eta)$ -plots in this computational scheme correspond to every one hundredth time step, as little happens during the intervals between. There is, however, an exception. During the first interval of 100 time steps, transients occur in the simulation as the probability fluctuates on short times, reflecting the finite iteration depth. It should be emphasized that plots of  $G(\eta)$  are in principle time invariant, depending on the similarity variable  $\eta$  and not  $t$ . Initial transients in this sense are only a reflection of the departure of the model lattice from the true fractal. In figure 6 a fibre and data corresponding

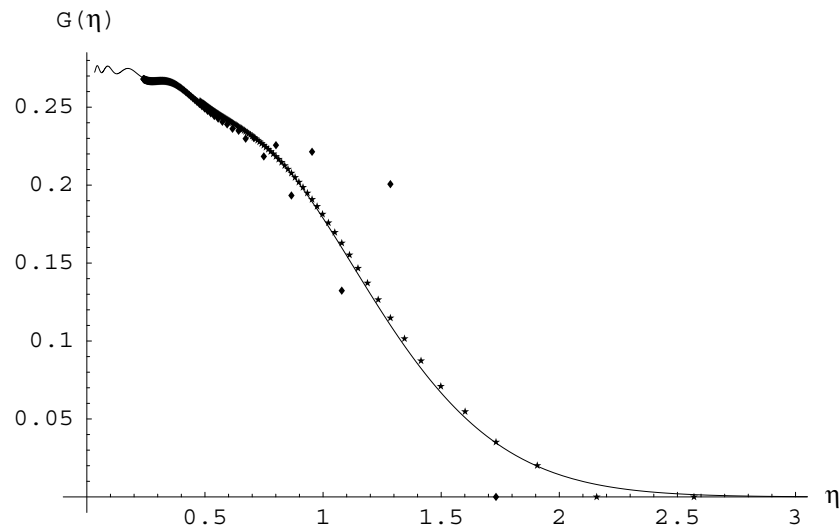


**Figure 6.** Transients for  $x_6$  (stars) and  $x_7$  (diamonds) relaxing to the fibre created by the set  $\{x_k\}$  (represented by the solid curve). Since  $x_7$  is nearer to the starting point in figure 4, probability arrives earlier there, which results in a larger deviation from the fibre for small times.

to particular echo points, within such transient intervals of the first 100 time steps, are plotted together.

To interpret this plot, it is important to note that, for  $r$  fixed,  $\eta$  decreases with increasing  $t$ . Thus the transients die out as the sequence of points advances *leftward*. Note that these sequences clearly relax to the fibre (represented by a solid curve) confirming that fibres have a computationally invariant quality. They even relax to the wiggles, indicating that the fibre's wiggles should not be confused with transient fluctuations but instead are real features of the invariant function that the computed sequence approaches. In this regard, it should also be emphasized that in figure 5 there are 100 time steps between data for the whole fibre, while there is only *one* time step between data points for the transient sequences in figure 6.

The fibre exists in principle from  $\eta$  equals zero to infinity. However, in the calculation all sequences for each individual gasket point begins at finite  $\eta$  and ends before zero. That is because the practical computation has a lower length scale and runs for a finite number of time steps. For any given member of an echo class, matching the fibre over a wider interval requires longer times or smaller scales. Smaller scales implies more points between starting point and the given member in question. However, smaller scales are unnecessary in practice as the echo points permit the fibre to be determined over the whole range of interest by simply choosing appropriate points in the same echo class having larger values of  $r$ .

After establishing the nature of the fibres as continuous single-valued functions that are invariant across an echo class, we can return to figure 3 to consider the envelope defining the muscle due to the behaviour of the fibres. Careful examination shows that no single fibre corresponds to the envelope, but that the envelope is instead formed by segments of successive fibres. Furthermore the wiggles evidently cause some fibres to touch the envelope on both sides of the muscle.

These fibres, which are continuous functions, and the muscle defining a family of functions, are natural objects to examine with differential equations, in contrast to the fractal PDFs, which have been unsuccessfully treated previously with them. In a future paper we will investigate



the possibility that the fibres are described by ordinary or extraordinary (i.e. fractional) DEs, and attempt to retrieve the evolution equation for the  $GDF$  of random walkers on a fractal in that way.

This new approach toward diffusion on fractals in terms of fibres also introduces a new approach to averaging for PDFs. A computation of a single ‘collective’  $GDF$  may be in terms of an average of the point cloud, which will be a weighted average of the fibres. That is in  $G - \eta$  space averaging is implicitly over functions of  $\eta$ . A density of states calculation which explicitly considers the relative importance of the various echo point sets to the construction of the fractal object will be needed. We will also investigate this question in a future paper.

## References

- [1] O’Shaughnessy B and Procaccia I 1985 *Phys. Rev. Lett.* **54** 455
- [2] Giona M and Roman H E 1992 *Physica A* **185** 87  
Roman H E and Giona M 1992 *J. Phys. A: Math. Gen.* **25** 2107
- [3] Metzler R, Glöcke W G and Nonnenmacher T F 1994 *Physica A* **211** 13
- [4] Compte A and Jou D 1996 *J. Phys. A: Math. Gen.* **29** 4321
- [5] Schulzky C, Essex C, Davison M, Franz A and Hoffmann K H 2000 *J. Phys. A: Math. Gen.* **33** 5501
- [6] Schubert S 1999 Random walks in complex systems—anomalous relaxation *PhD Thesis* TU Chemnitz, Germany
- [7] Hoffmann K H, Essex C and Schulzky C 1998 *J. Non-Equilib. Thermodyn.* **23** 166
- [8] Klafter J, Zumofen G and Blumen A 1991 *J. Phys. A: Math. Gen.* **24** 4835
- [9] Sornette D 1998 *Phys. Rep.* **297** 239
- [10] Schulzky C 2000 Anomalous diffusion and random walks on fractals *PhD Thesis* TU Chemnitz, Germany